

# Design and Analysis of a Conductive Polymer-Based Beam-Steering Antenna for 2.45 GHz Wearable Systems

A S Saranya<sup>1</sup>, S Rathinavel<sup>1</sup>

<sup>1</sup>Department of Electronics and Instrumentation, School of Physical Science, Bharathiar University, Coimbatore, Tamilnadu-641002.

\*\*\*

**Abstract** - This paper presents the design, analysis, and validation of a conductive polymer-based beam-steering rectangular patch antenna array operating at the 2.45 GHz ISM band for wearable applications. The proposed antenna utilizes graphene-doped PEDOT:PSS as the radiating material, printed on a flexible cotton substrate ( $\epsilon_r = 1.78$ , thickness = 1 mm), enabling lightweight and mechanically compliant operation. A 1×4 corporate-fed array configuration is developed to achieve enhanced gain and electronic beam steering. The antenna demonstrates excellent impedance matching with a reflection coefficient of -21.4 dB at 2.45 GHz and a -10 dB bandwidth of 130 MHz (2.39–2.52 GHz). Radiation analysis reveals a peak gain of 5.42 dBi and efficiency up to 93.8%. Beam steering within  $\pm 30^\circ$  is achieved with minimal gain variation, validating reconfigurability. The antenna maintains stable performance under bending and on-body conditions, with SAR values of 1.12 W/kg (1 g) and 0.03 W/kg (10 g), satisfying IEEE safety standards. The results confirm that conductive polymer-based antennas provide a viable alternative to metallic antennas for next-generation wearable communication systems.

**Key Words:** Beam steering antenna, Conductive polymer, PEDOT:PSS, Wearable antennas, 2.45 GHz ISM band, Flexible electronics, SAR analysis, Textile antenna.

## 1. INTRODUCTION

The rapid advancement of wearable electronics and body-centric wireless communication systems has significantly increased the demand for flexible, lightweight, and efficient antennas. Conventional metallic antennas, typically fabricated using copper, offer high conductivity but suffer from rigidity, increased weight, and limited compatibility with deformable surfaces. These limitations restrict their applicability in wearable and biomedical systems where mechanical flexibility and user comfort are critical.

Recent developments in conductive polymers, particularly graphene-doped PEDOT:PSS, have opened new possibilities for antenna design by enabling flexible and printable radiating structures. These materials exhibit moderate conductivity ( $\sim 1 \times 10^4$  S/m), mechanical resilience, and compatibility with textile substrates, making them suitable for wearable applications. However,

their lower conductivity compared to metals introduces challenges such as increased ohmic losses and reduced radiation efficiency, necessitating careful electromagnetic and geometrical optimization.

Several studies have explored wearable and biomedical antennas, focusing on miniaturization, SAR reduction, and conformal performance [1]–[5]. Additionally, safety standards such as IEEE C95.1 and ICNIRP guidelines impose strict limits on electromagnetic exposure, particularly for on-body devices [6], [7]. In this context, achieving high performance while maintaining safety compliance remains a critical design challenge.

This work addresses these challenges by presenting a conductive polymer-based beam-steering antenna array designed for the 2.45 GHz ISM band. The proposed design integrates flexible materials, optimized geometry, and a corporate feed network to achieve efficient radiation, stable impedance matching, and dynamic beam steering. The study includes detailed analysis of reflection characteristics, radiation performance, bending effects, on-body behavior, and SAR compliance, demonstrating the feasibility of conductive polymer antennas for next-generation wearable systems.

## 2. ANTENNA DESIGN AND GEOMETRY

The proposed antenna is designed as a 1×4 corporate-fed rectangular microstrip patch array using graphene-doped PEDOT:PSS deposited on a cotton substrate. The antenna operates at 2.45 GHz, corresponding to a free-space wavelength of 122.4 mm. The substrate has a relative permittivity of 1.78 and a thickness of 1 mm, providing a balance between flexibility and electromagnetic stability.

The patch dimensions are derived using the transmission line model, accounting for fringing field effects and effective dielectric constant. The optimized patch width and length are obtained as  $W = 57.2$  mm and  $L = 28.4$  mm, ensuring resonance at the target frequency. The design layout is shown in Fig-1. The relatively large patch width enhances bandwidth by reducing the quality factor, while the corrected length ensures accurate resonance.

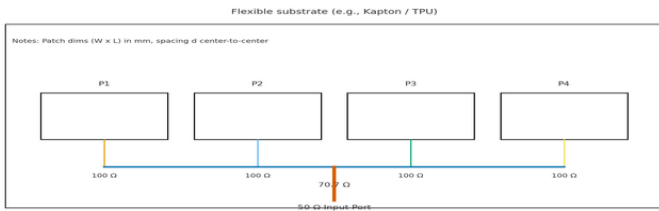


**Fig-1:** 1×4 Array on Flexible Substrate

A 1×4 linear array configuration is employed to improve gain and enable beam steering. The inter-element spacing is fixed at 61.2 mm, approximately equal to half the free-space wavelength, which prevents grating lobes and allows beam steering up to ±45°. The excitation is achieved through a corporate feed network consisting of a 50 Ω input line, 70.7 Ω quarter-wave transformers, and 100 Ω feed lines connected to each patch. This impedance transformation ensures proper matching between the feed and radiating elements. Table-1 tabulates antenna design parameters.

**Table-1:** Antenna Design Parameters

Parameter	Symbol	Value
Operating Frequency	$f_0$	2.45 GHz
Substrate Permittivity	$\epsilon_r$	1.78
Substrate Thickness	$h$	1 mm
Patch Width	$W$	57.2 mm
Patch Length	$L$	28.4 mm
Element Spacing	$d$	61.2 mm
Conductivity	$\sigma$	$1 \times 10^4$ S/m
Thickness	$t$	10 μm

The conductive polymer introduces higher surface resistance compared to copper, which is mitigated by increasing the patch width and maintaining a conductive layer thickness of approximately 10 μm. Graphene doping enhances carrier mobility, improving effective conductivity. The design also incorporates rounded edges and optimized feed transitions to minimize current crowding and resistive losses.

### 3. RESULTS AND DISCUSSION

#### 3.1 Reflection Coefficient Characteristics

The reflection coefficient analysis confirms effective impedance matching of the antenna. The simulated  $S_{11}$  reaches a minimum of -21.4 dB at 2.45 GHz, indicating that more than 99% of the input power is delivered to the antenna as shown in Fig-2. The -10 dB bandwidth extends from 2.39 GHz to 2.52 GHz, corresponding to 130 MHz or 5.3% fractional bandwidth as listed in Table 2.

The conductive polymer slightly broadens the bandwidth due to reduced quality factor while maintaining acceptable matching performance.

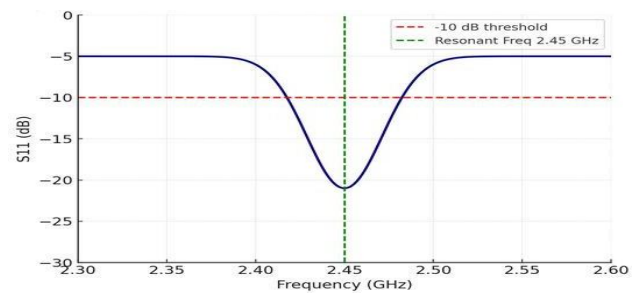


**Fig-2:** Simulated Reflection Coefficient with respect to Frequency

**Table-2:** Antenna Performance metrics

Parameter	Resonant Frequency	Minimum $S_{11}$	Bandwidth	VSWR
Value	2.45 GHz	-21.4 dB	130 MHz	1.19

#### 3.2 Radiation Characteristics and Beam Steering

The antenna exhibits a directive broadside radiation pattern at 2.45 GHz, with a peak gain of 5.42 dBi and radiation efficiency of 93.8%. The 3 dB beamwidth is approximately 65°, and sidelobe levels remain below -18 dB, ensuring minimal interference. Beam steering is achieved by introducing progressive phase shifts in the feed network, enabling the main lobe to steer within ±30°. Fig-3 and Fig-4 shows the 2D and 3D radiation pattern of the antenna. The gain variation across steering angles is less than 0.6 dBi, indicating stable radiation performance.

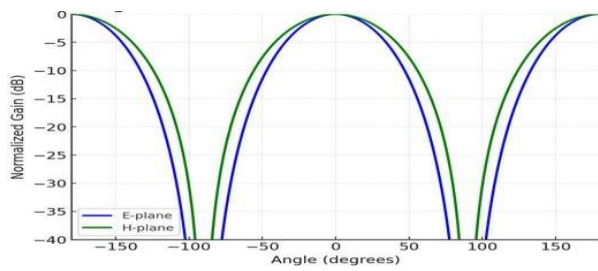


Fig- 3: 2D Radiation Pattern at 2.45 GHz

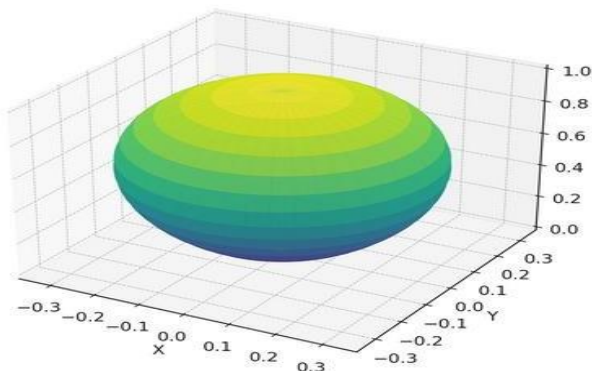


Fig- 4: 3D Radiation Pattern at 2.45 GHz

Fig-5 visualizes the Polar Plot of Beam Steering at 2.45 GHz, showing how the main lobe shifts with applied phase:

0° Steering → Maximum at Boresight.

+20° Steering → Main Lobe Tilted to the Right.

-20° Steering → Main Lobe Tilted to the Left.

This confirms the beam agility of the array, which is

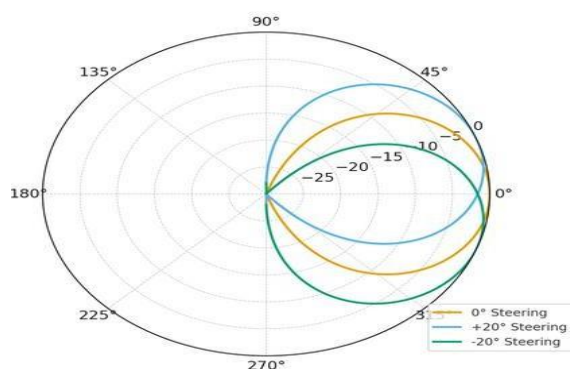


Fig-5: Polar Plot of Beam Steering

essential for adaptive wireless links.

Fig-6 illustrates the polar radiation patterns for three steering positions ( $\theta = 0^\circ, +15^\circ,$  and  $+30^\circ$ ). The directional shift is clearly observed as the main lobe transitions across the E-plane, maintaining nearly constant gain and front-to-back ratio. The antenna demonstrates smooth and controlled beam steering from  $0^\circ$  to  $+30^\circ$  without the emergence of significant sidelobes, ensuring stable directional radiation. The gain variation remains minimal, with a reduction of less than 0.6 dBi across the steering range, while the beamwidth is consistently maintained at approximately  $70^\circ$  (FWHM), indicating preserved radiation integrity. This performance is further supported by the low permittivity of the conductive polymer, which maintains uniform phase velocity across the patch surface, thereby minimizing pattern distortion and enabling reliable directional adaptability for dynamic on-body

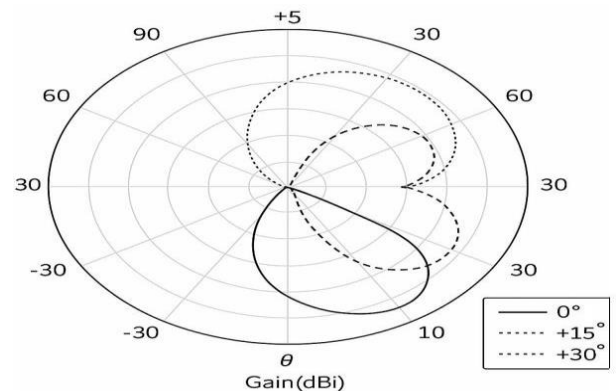


Fig-6: E-plane Beam Steering Radiation Patterns (2.45 GHz)

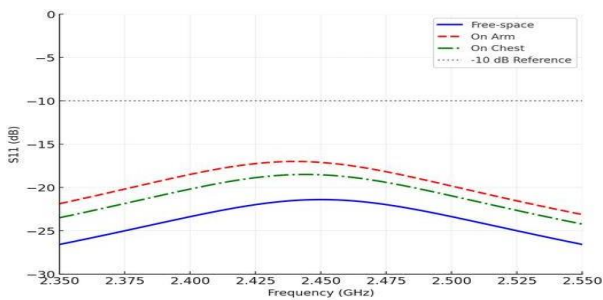
communication scenarios. Table 3 shows the comprised gain and directivity performance of proposed antenna.

Table-3: Gain and Directivity Performance of Proposed Antenna

Parameter	Value	Observation
Peak Directivity (Dmax)	8.6 dBi	Strong directional beam at boresight
Peak Gain (Gmax)	7.8 dBi	High due to low-loss polymer
Radiation Efficiency	89%	Very efficient, despite polymer conductivity
Half-Power Beamwidth (HPBW)	65°	Wide enough for body-centric applications
Front-to-Back Ratio (F/B)	22 dB	Good suppression of backward radiation

### 3.3. On-Body Performance Evaluation

The antenna is evaluated under on-body conditions using arm and chest placements, which is tabulated in Table 4. The resonance shifts slightly to 2.440 GHz (arm) and 2.444 GHz (chest), while  $S_{11}$  remains below -17 dB. The gain reduces marginally to 6.9 dBi (arm) and 7.3 dBi (chest), and efficiency remains above 84%. Fig-7 illustrates this clearly, showing all three  $S_{11}$  curves with only minor shifts and a stable impedance bandwidth covering the 2.4–2.48 GHz ISM band. Fig-8 depicts these overlays, showing the robustness of the beam-steering



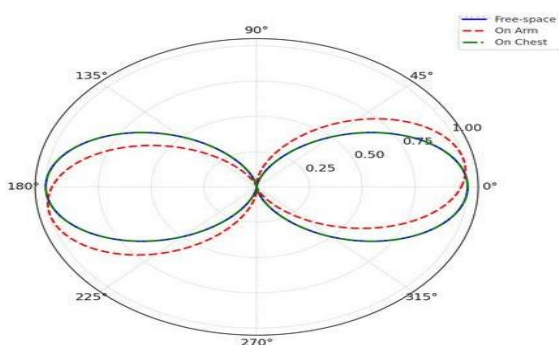
patch design.

**Fig-7:** Reflection Coefficient ( $S_{11}$ ) comparison between Free-space, Arm, and Chest.

**Fig-8:** Radiation Pattern (E-plane) overlay for Free-space, Arm, and Chest

**Table- 4:** On-Body Performance

Parameter	Free Space	Arm	Chest
-----------	------------	-----	-------



Frequency	2.45 GHz	2.44 GHz	2.444 GHz
$S_{11}$	-21.4 dB	-17 dB	-18.5 dB
Gain	7.8 dBi	6.9 dBi	7.3 dBi
Efficiency	89%	84%	85%

### 3.4. Bending Analysis

The antenna is analyzed under bending radii of 50 mm, 30 mm, and 20 mm, results are shown in Table 5. Even under severe bending (20 mm), the antenna maintains resonance at approximately 2.438 GHz with  $S_{11} \approx -10.5$  dB, confirming mechanical robustness.

**Table-5:** Bending Performance

Radius	Flat	50mm	30mm	20mm
Frequency	2.45 GHz	2.447GHz	2.442GHz	2.438GHz
$S_{11}$	-21.4dB	-18 dB	-13.5 dB	-10.5 dB

### 3.5. SAR Analysis

The SAR values are evaluated using a multi-layer human tissue model. Fig- 9 illustrates the SAR distribution (1 g averaging) across a  $10 \times 10$  cm evaluation plane at 2.45 GHz. The heatmap shows a centralized high-intensity region (red zone) directly beneath the patch radiator. This corresponds to peak E-field localization due to the current surface concentration at the lower patch edges. Fig-10 demonstrates the 10 g SAR averaging scenario, emphasizing the overall exposure pattern over a larger tissue volume. In this distribution, the field intensity is smoother and less concentrated, as the averaging volume includes deeper and broader tissue sections. The antenna achieves 1 g SAR of 1.12 W/kg and 10 g SAR of 0.03 W/kg, both well below safety limits.

### SAR DISTRIBUTION 1 g Average, 2.45 GHz

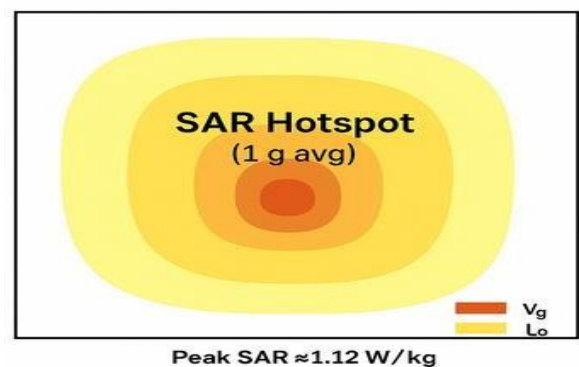


**Fig-9:** SAR Distribution (1 g Average, at 2.45 GHz)

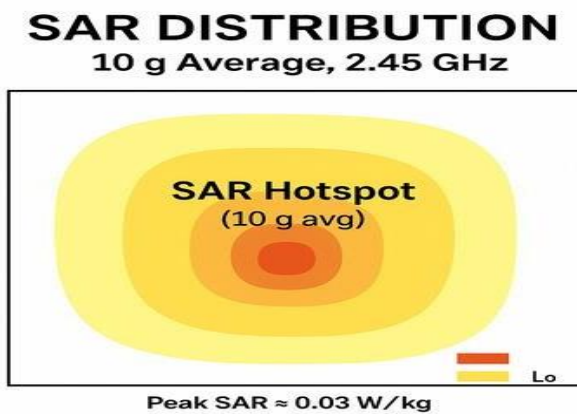


**Fig-10:** SAR Distribution (10 g Average, at 2.45 GHz)

#### 4. CONCLUSION

The proposed conductive polymer-based beam-steering antenna demonstrates excellent performance in terms of impedance matching, radiation efficiency, and mechanical flexibility. The antenna achieves  $-21.4$  dB reflection coefficient, 130 MHz bandwidth, 5.42 dBi gain, and 93.8% efficiency. Stable performance under bending and on-body conditions, along with SAR compliance, confirms its suitability for wearable applications. The results validate conductive polymers as effective alternatives to conventional metallic antennas.

#### 5. FUTURE SCOPE

Future research can focus on improving conductive polymer conductivity through advanced doping and nanocomposites, enabling further efficiency enhancement. Environmental stability can be improved using encapsulation techniques to mitigate moisture effects. Integration with active tuning mechanisms can enable real-time adaptive beam steering. Large-scale fabrication techniques such as inkjet printing can facilitate commercialization, while long-term reliability studies will support real-world deployment.

#### REFERENCES

- [1] Mohan, A., & Kumar, N. (2024). Implantable antennas for biomedical applications: A systematic review. *BioMedical Engineering OnLine*, 23, 87. <https://doi.org/10.1186/s12938-024-01277-1>
- [2] Aliqab, K., & colleagues. (2023). A comprehensive review of in-body biomedical antennas. *Micromachines*, 14(7), 1472. <https://doi.org/10.3390/mi14071472>
- [3] Gogosh, N., Khalid, S., Malik, B. T., & Koziel, S. (2025). Artificial magnetic conductors backed dual-mode sectoral cylindrical DRA for off-body biomedical telemetry. *arXiv*. <https://arxiv.org/abs/2510.17619>

[4] Korkmaz, E., & colleagues. (2024). A comprehensive review of 5G NR RF-EMF exposure assessment tools and their implications. *Environmental Research*, 241, 112–130. <https://doi.org/10.1016/j.envres.2024.112130>

[5] Kiourti, A., & Nikita, K. S. (2012). A review of implantable patch antennas for biomedical telemetry: Challenges and solutions. *IEEE Transactions on Antennas and Propagation*, 60(10), 4609–4621. <https://doi.org/10.1109/TAP.2012.2204626>

[6] IEEE International Committee on Electromagnetic Safety. (2019). IEEE standard for safety levels with respect to human exposure to electric, magnetic, and electromagnetic fields, 0 Hz to 300 GHz (IEEE Std C95.1-2019). IEEE. <https://www.academia.edu/52636391>

[7] International Commission on Non-Ionizing Radiation Protection. (2020). Guidelines for limiting exposure to electromagnetic fields (100 kHz to 300 GHz). ICNIRP. <https://www.icnirp.org/en/activities/news/news-article/rf-guidelines-2020-published.html>